First-order analysis of a two-conjugate zoom system

Mau-Shiun Yeh
National Chiao Tung University
Institute of Electro-Optical Engineering
1001 Ta Hsueh Road
Hsin Chu 30050, Taiwan

Shin-Gwo Shiue
Industrial Technology Research Institute
Opto-Electronics & Systems Laboratories
Q000 OES/ITRI
Building 44, 195-8 Chung Hsing Road, Section 4
Chutung, Hsin Chu, 310, Taiwan

Mao-Hong Lu, MEMBER SPIE
National Chiao Tung University
Institute of Electro-Optical Engineering
1001 Ta Hsueh Road
Hsin Chu 30050, Taiwan
E-mail: mhlu@jenny.nctu.edu.tw

Abstract. A general analysis for the first-order design of the two-conjugate zoom system, which consists of three lenses and has a real or virtual image, is presented. The design formulas are derived. Of two-conjugate zoom systems, we analyze the solution areas in the system parameter diagrams under two particular initial conditions in which the object/image and pupil magnifications of the middle lens are taken to be 1 and -1 or -1 and 1. Two design methods are proposed. Several examples are given to demonstrate the proposed design procedures.

Subject terms: two-conjugate zoom lenses.

Paper 08026 received Feb. 13, 1996; revised manuscript received May 18, 1996; accepted for publication May 20, 1996.

1 Introduction

A zoom system is generally considered to consist of three parts: the focusing, zooming, and fixed parts. The focusing part is placed in front of the zooming part, to adjust the object distance. The zooming part is literally used for zooming and the fixed rear part serves to control the focal length or magnification and reduce the aberrations of the whole system. Some published papers[1] concentrate on the first-order zoom design in which only the object/image distance is fixed. However, few of them discuss the possible solutions in the first-order design. Oskotsky[2] describes a graphoanalytical method for the first-order design of two-lens zoom systems and discusses the region of Gaussian solution. Johnson and Feng[3] use a methodology to discuss the potential solutions for a mechanically compensated zoom lenses with a single moving element. We have also proposed a two-optical-component method for designing zoom system.[4]

In a general zoom system, the aperture stop is usually placed after the moving elements and before a fixed lens, so the exit pupil position is fixed but the entrance pupil position varies widely in zooming. In some optical systems, the wandering of the entrance pupil is not a great disadvantage. However, the variation of the entrance pupil position could be a very serious disadvantage for a large-zoom-ratio system or a zoom-phase-contrast microscope.

A two-conjugate zoom system is the one in which not only the object and image but also the entrance and exit pupils are fixed during zooming. Such a zoom system requires at least three lenses that move separately. Hopkins[5] proposed the first-order design formulas for a special symmetrical two-conjugate zoom system. In that case, the powers of the first and third lenses are the same and the middle lens has a power with an opposite sign; the distance from object to entrance pupil and the distance from image to exit pupil are equal, but in opposite direction; the object/image and pupil magnifications are numerically reciprocal and in opposite sign; and the power of the system is the same for any given magnification and its reciprocal. In the mean position of zooming, he assumes the system has object/image magnification $M=-1$ and pupil magnification $M=1$, and the magnification of the middle lens M_2 is -1. Following the method described by Hopkins, Shiue[6] discussed the two-conjugate zoom system with $M=1$, $M=-1$, and $M_2=1$ in the mean position of zooming.

In this paper, we analyze a general two-conjugate zoom system that consists of three lenses and has a real or virtual image. The powers of the three lenses and the positions of object, image, entrance, and exit pupils are not constrained as those in the symmetrical system proposed by Hopkins.[5] To simplify the design, we discuss two special two-conjugate zoom systems in which the object/image and pupil magnifications of the middle lens at the initial condition are 1 and -1 or -1 and 1. In both cases, we find the possible solutions for the positions of object, image, entrance, and exit pupils, which are related to the power values of the three lenses, with the graphoanalytical method.[2] Two design methods are discussed. Four examples are presented to demonstrate this analysis.

2 Theory

2.1 *General Design Formulas*

The notation used in this paper is shown in Fig. 1. The object O is imaged at O' with a object/image magnification M and the entrance pupil E is imaged at the exit pupil E' with a pupil magnification M. Here ℓ and ℓ' are the distances from the first principal plane to the object and the

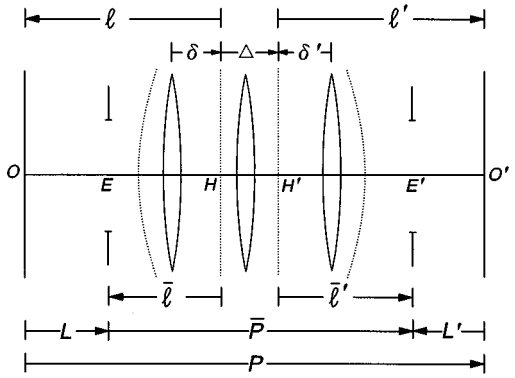

Fig. 1 Diagram of the Gaussian optics: P and $\bar{P}$ are the distance from object to image and the distance from entrance to exit pupil, respectively.

second principal plane to the image, respectively. Similarly, ℓ and ℓ' are the distances from the first principal plane to the entrance pupil and the second principal plane to the exit pupil. In this paper, the distance to the right of the reference point is positive; that to the left is negative. In this analysis, we take the paraxial and thin-lens approximations. For a thin lens, both the principal planes coincide with the lens. The general conjugate equation gives

$$\frac{M}{L'}-\frac{1}{ML}=K=\frac{1}{F}, \tag{1}$$

where K and F are the equivalent power and focal length of the system, respectively; $L=(OE)$ is the distance from object to entrance pupil of the system; and $L'=(O'E')$ is the distance from image to exit pupil of the system. From Gaussian optics, we have

$$L=\bar{\ell}-\ell=\left(\frac{1}{\bar{M}}-\frac{1}{M}\right)F, \tag{2}$$

$$L'=\bar{\ell}'-\ell'=(M-\bar{M})F. \tag{3}$$

With the distance from the first to the second principal plane, $\Delta=(HH')$, we have

$$K\Delta=PK-\left(2-M-\frac{1}{M}\right), \tag{4}$$

where P is the distance from object to image (OO').

For a three-lens system with powers K_1, K_2, and K_3 and interlens separations d_{12} and d_{23}, the power K and the distance Δ are given by

$$K=K_1+K_2+K_3-dK_1K_3-(d_{12}K_1+d_{23}K_3)K_2 + d_{12}d_{23}K_1K_2K_3, \tag{5}$$

$$K\Delta=-d^2K_1K_3-(d_{12}^2K_1+d_{23}^2K_3)K_2+dd_{12}d_{23}K_1K_2K_3, \tag{6}$$

where $d=d_{12}+d_{23}$. Here, d_{12} can be expressed as

$$d_{12}=\ell_1'-\ell_2=(1-M_1)F_1-\left(\frac{1}{M_2}-1\right)F_2, \tag{7}$$

$$\text{or}\quad d_{12}=\bar{\ell}_1'-\bar{\ell}_2=(1-\bar{M}_1)F_1-\left(\frac{1}{\bar{M}_2}-1\right)F_2, \tag{8}$$

where $M_1(\bar{M}_1)$ and $M_2(\bar{M}_2)$ are the object/image (pupil) magnifications of the first and second lenses, respectively. Using Eqs. (7) and (8), we have

$$F_2=-\frac{M_1-\bar{M}_1}{1/M_2-1/\bar{M}_2}F_1. \tag{9}$$

Similarly, d_{23} can be expressed as

$$d_{23}=\ell_2'-\ell_3=(1-M_2)F_2-\left(\frac{1}{M_3}-1\right)F_3, \tag{10}$$

$$\text{or}\quad d_{23}=\bar{\ell}_2'-\bar{\ell}_3=(1-\bar{M}_2)F_2-\left(\frac{1}{\bar{M}_3}-1\right)F_3. \tag{11}$$

From Eqs. (10) and (11), we have

$$F_3=-\frac{M_2-\bar{M}_2}{1/M_3-1/\bar{M}_3}F_2. \tag{12}$$

Note that L and L' can also be regarded as the distances from object to entrance pupil of the first lens and from image to exit pupil of the third lens, respectively. So we have

$$L=\bar{\ell}_1-\ell_1=\left(\frac{1}{\bar{M}_1}-\frac{1}{M_1}\right)F_1 \tag{13}$$

and

$$L'=\bar{\ell}_3'-\ell_3'=(M_3-\bar{M}_3)F_3. \tag{14}$$

From Eqs. (1) to (6) with different values of K_1, K_2, and K_3, we can obtain a zoom system. However, it is difficult to get a satisfactory result by generally solving the preceding equations. To get a desirable solution easily, some constraints in solving are needed.

2.2 *Two Special Initial Conditions*

As mentioned, the special initial conditions in which the object/image magnification M_2 and pupil magnification M_2 of the middle lens are 1 and -1 or -1 and 1 in the initial position are assumed. In the following, we discuss the solutions under these two initial conditions.

2.2.1 *Case 1: $M_2=1$ and $\bar{M}_2=-1$*

In this case, the marginal ray is through the center of the middle lens, as shown in Fig. 2. Substituting $M_2=1$ and $M_2=-1$ into Eqs. (9) and (12), we have

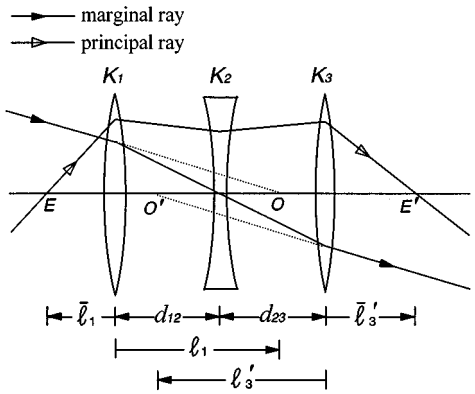

Fig. 2 Three-lens zoom system with the initial conditions $M_2=1$ and $M_2=-1$. The marginal ray is through the center of the middle lens.

$$F_2=-\frac{M_1-\overline{M_1}}{2}F_1, \tag{15}$$

$$F_3=-\frac{2}{1/M_3-1/\overline{M_3}}F_2. \tag{16}$$

In paraxial approximation, we have

$$\ell_1=\left(\frac{1}{M_1}-1\right)F_1, \tag{17}$$

$$\overline{\ell_1}=\left(\frac{1}{\overline{M_1}}-1\right)F_1, \tag{18}$$

$$\ell'_3=(1-M_3)F_3 \tag{19}$$

$$\overline{\ell'_3}=(1-\overline{M_3})F_3. \tag{20}$$

Equations (17) to (20) indicate the positions of object, entrance pupil, image, and exit pupil. From these equations, we find that the positions of two pairs of conjugate planes are related to the values of F_1, F_2, and F_3, and the values of object/image and pupil magnifications of each lens.

Substituting the initial condition, $M_2=1$ and $M_2=-1$, into Eqs. (7), (8), (10), and (11) and using Eqs. (18) and (20), we get

$$d_{12}=(1-M_1)F_1, \tag{21}$$

$$d_{12}=(1-\overline{M_1})F_1+2F_2, \tag{22}$$

Table 1 Solution ranges of object position ℓ_1 for different types of F_1 with the initial conditions $M_2=1$ and $M_2=-1$.

Types of F_1	Solution Ranges of ℓ_1
$F_1>0$	$(\ell_1+F_1)>F_1$ or $(\ell_1+F_1)<0$
$F_1<0$	$F_1<(\ell_1+F_1)<0$

Table 2 Solution ranges of entrance pupil position $\overline{\ell_1}$ for different combinations of F_1 and F_2 with the initial conditions $M_2=1$ and $M_2=-1$.

Types of F_1 and F_2		Solution Ranges of $\overline{\ell_1}$
$F_1>0$, $F_2>0$		$(\overline{\ell_1}+F_1)>\frac{F_1^2}{F_1+2F_2}>0$ or $(\overline{\ell_1}+F_1)<0$
$F_1>0$, $F_2<0$	$F_1+2F_2>0$	$(\overline{\ell_1}+F_1)>\frac{F_1^2}{F_1+2F_2}>0$ or $(\overline{\ell_1}+F_1)<0$
	$F_1+2F_2=0$	$(\overline{\ell_1}+F_1)<0$
	$F_1+2F_2<0$	$\frac{F_1^2}{F_1+2F_2}<(\overline{\ell_1}+F_1)<0$
$F_1<0$, $F_2>0$	$F_1+2F_2>0$	$(\overline{\ell_1}+F_1)>\frac{F_1^2}{F_1+2F_2}>0$ or $(\overline{\ell_1}+F_1)<0$
	$F_1+2F_2=0$	$(\overline{\ell_1}+F_1)<0$
	$F_1+2F_2<0$	$\frac{F_1^2}{F_1+2F_2}<(\overline{\ell_1}+F_1)<0$
$F_1<0$, $F_2<0$		$\frac{F_1^2}{F_1+2F_2}<(\overline{\ell_1}+F_1)<0$

$$d_{12}=-\frac{F_1^2}{\overline{\ell_1}+F_1}+(F_1+2F_2), \tag{23}$$

$$d_{23}=-\left(\frac{1}{M_3}-1\right)F_3, \tag{24}$$

$$d_{23}=2F_2-\left(\frac{1}{\overline{M_3}}-1\right)F_3, \tag{25}$$

$$d_{23}=\frac{F_3^2}{\overline{\ell'_3}-F_3}+(F_3+2F_2). \tag{26}$$

The interlens separations d_{12} and d_{23} must be positive in zooming. This provides some constraints on the solution, i.e., on ℓ_1, $\overline{\ell_1}$, ℓ'_3, and $\overline{\ell'_3}$. Under these constraints, we can calculate the solution ranges of ℓ_1 and ℓ'_3 with Eqs. (17), (19), (21), and (24). From Eq. (23), we can also find the solution ranges of ℓ_1 for different combinations of F_1 and F_2. Similarly, from Eq. (26) we obtain the solution ranges of $\overline{\ell'_3}$ for different combinations of F_2 and F_3. All the results for ℓ_1 and $\overline{\ell_1}$ are shown in Tables 1 and 2 and for ℓ'_3 and $\overline{\ell'_3}$ in Tables 3 and 4.

By using Eqs. (15), (18), and (21), $F_1^2/(F_1+2F_2)$ in Table 2 becomes

Table 3 Solution ranges of image position ℓ'_3 for different types of F_3 with the initial conditions $M_2=1$ and $M_2=-1$.

Types of F_3	Solution Ranges of ℓ'_3
$F_3>0$	$(\ell'_3-F_3)>0$ or $(\ell'_3-F_3)<-F_3$
$F_3<0$	$-F_3>(\ell'_3-F_3)>0$

$$\frac{F_1^2}{F_1+2F_2}=\frac{\overline{\ell}_1+F_1}{1+[(1-M_1)F_1/F_1^2](\overline{\ell}_1+F_1)}$$
$$=\frac{(\overline{\ell}_1+F_1)}{1+(d_{12}/F_1^2)(\overline{\ell}_1+F_1)}. \quad (27)$$

Here d_{12} must be positive. The value of $1+d_{12}(\overline{\ell}_1+F_1)/F_1^2$ is greater than 1 if $\ell_1+F_1>0$ and is between 0 and 1 if $\ell_1+F_1<0$ and $F_1+2F_2<0$, so the inequality equation $\ell_1+F_1>F_1^2/(F_1+2F_2)$ in Table 2 is always true. It means that the constraints $\ell_1+F_1>F_1^2/(F_1+2F_2)>0$ and $F_1^2/(F_1+2F_2)<\ell_1+F_1<0$ are actually equivalent to the conditions $\ell_1+F_1>0$ and $\ell_1+F_1<0$, respectively.

By using Eqs. (16), (20), and (24), the term $-F_3^2/(F_3+2F_2)$ in Table 4 becomes

$$\frac{-F_3^2}{F_3+2F_2}=\frac{(\overline{\ell}'_3-F_3)}{1-[-(1/M_3-1)F_3/F_3^2](\overline{\ell}'_3-F_3)}$$
$$=\frac{(\overline{\ell}'_3-F_3)}{1-(d_{23}/F_3^2)(\overline{\ell}'_3-F_3)}. \quad (28)$$

Here d_{23} must be positive. The value of $1-d_{23}(\overline{\ell}'_3-F_3)/F_3^2$ is greater than 1 if $\overline{\ell}'_3-F_3<0$ and is between 0 and 1 if $\overline{\ell}'_3-F_3>0$ and $F_3+2F_2<0$, so the inequality equation $-F_3^2/(F_3+2F_2)>\overline{\ell}'_3-F_3$ in Table 4 is always true. It means that the constraints $\overline{\ell}'_3-F_3<-F_3^2/(F_3+2F_2)<0$ and $-F_3^2/(F_3+2F_2)>\overline{\ell}'_3-F_3>0$ are actually equivalent to the conditions $\overline{\ell}'_3-F_3<0$ and $\overline{\ell}'_3-F_3>0$, respectively.

By using Eqs. (15), (17), and (18), the term F_1+2F_2 in Table 2 can also be written as

$$F_1+2F_2=F_1-\frac{(\overline{\ell}_1+F_1)-(\ell_1+F_1)}{(\ell_1+F_1)(\ell_1+F_1)}F_1^2. \quad (29)$$

The curve for $F_1+2F_2=0$ is a hyperbola in the $\ell_1\sim\overline{\ell}_1$ diagram. The solution distribution in the diagram is thus divided into several areas by the hyperbolic curves and the sign of F_1+2F_2.

By using Eqs. (16), (19), and (20), F_3+2F_2 in Table 4 can be expressed as

$$F_3+2F_2=F_3+\frac{(\overline{\ell}'_3-F_3)-(\ell'_3-F_3)}{(\overline{\ell}'_3-F_3)(\ell'_3-F_3)}F_3^2. \quad (30)$$

Table 4 Solution ranges of exit pupil position $\overline{\ell}'_3$ for different combinations of F_2 and F_3 with the initial conditions $M_2=1$ and $M_2=-1$.

Types of F_2 and F_3		Solution Ranges of $\overline{\ell}'_3$
$F_3>0$, $F_2>0$		$(\overline{\ell}'_3-F_3)>0$ or $(\overline{\ell}'_3-F_3)<\frac{-F_3^2}{F_3+2F_2}<0$
$F_3>0$, $F_2<0$	$F_3+2F_2>0$	$(\overline{\ell}'_3-F_3)>0$ or $(\overline{\ell}'_3-F_3)<\frac{-F_3^2}{F_3+2F_2}<0$
	$F_3+2F_2=0$	$(\overline{\ell}'_3-F_3)>0$
	$F_3+2F_2<0$	$\frac{-F_3^2}{F_3+2F_2}>(\overline{\ell}'_3-F_3)>0$
$F_3<0$, $F_2>0$	$F_3+2F_2>0$	$(\overline{\ell}'_3-F_3)>0$ or $(\overline{\ell}'_3-F_3)<\frac{-F_3^2}{F_3+2F_2}<0$
	$F_3+2F_2=0$	$(\overline{\ell}'_3-F_3)>0$
	$F_3+2F_2<0$	$\frac{-F_3^2}{F_3+2F_2}>(\overline{\ell}'_3-F_3)>0$
$F_3<0$, $F_2<0$		$\frac{-F_3^2}{F_3+2F_2}>(\overline{\ell}'_3-F_3)>0$

Thus, $F_3+2F_2=0$ gives another hyperbola in the $\ell'_3\sim\overline{\ell}'_3$ diagram. Similarly, in this diagram, the solution distribution is thus divided into several areas by the hyperbolic curves and the sign of F_3+2F_2.

According to the different values of F_1, F_2, and F_3, we can illustrate the solution areas in the $\ell_1\sim\ell_1$ and $\ell'_3\sim\overline{\ell}'_3$ diagrams, as shown in Figs. 3 and 4, where we make coordinate transforms from $\ell_1(\ell_1)$ to $\ell_1+F_1(\ell_1+F_1)$ in the object (entrance pupil) space of the first lens and from $\ell'_3(\ell'_3)$ to $\ell'_3-F_3(\ell'_3-F_3)$ in the image (exit pupil) space of the third lens to make the magnifications have the same sign in each quadrant.

Figure 3 shows the solution areas of the object distance and entrance pupil distance of the first lens for different combinations of F_1 and F_2. Each solution area gives some constraints on the signs of the related parameters including F_1+2F_2, M_1, and M_1. From Eq. (15), the sign of (M_1-M_1) in each area is determined by the sign of F_2, which is given when the solution area is chosen. The sign of $L=(\ell_1-\ell_1)$, which is the distance from object to the entrance pupil, is positive in the upper-left section and negative in the lower-right section.

Similarly, Fig. 4 shows the solution areas of the image distance and exit pupil distance of the third lens for different combinations of F_2 and F_3. This figure shows the constraints on the signs of the related parameters, including F_3+2F_2, M_3, and M_3, in each solution area. Similar to L, the sign of $L'=(\overline{\ell}'_3-\ell'_3)$, which is the distance from im-

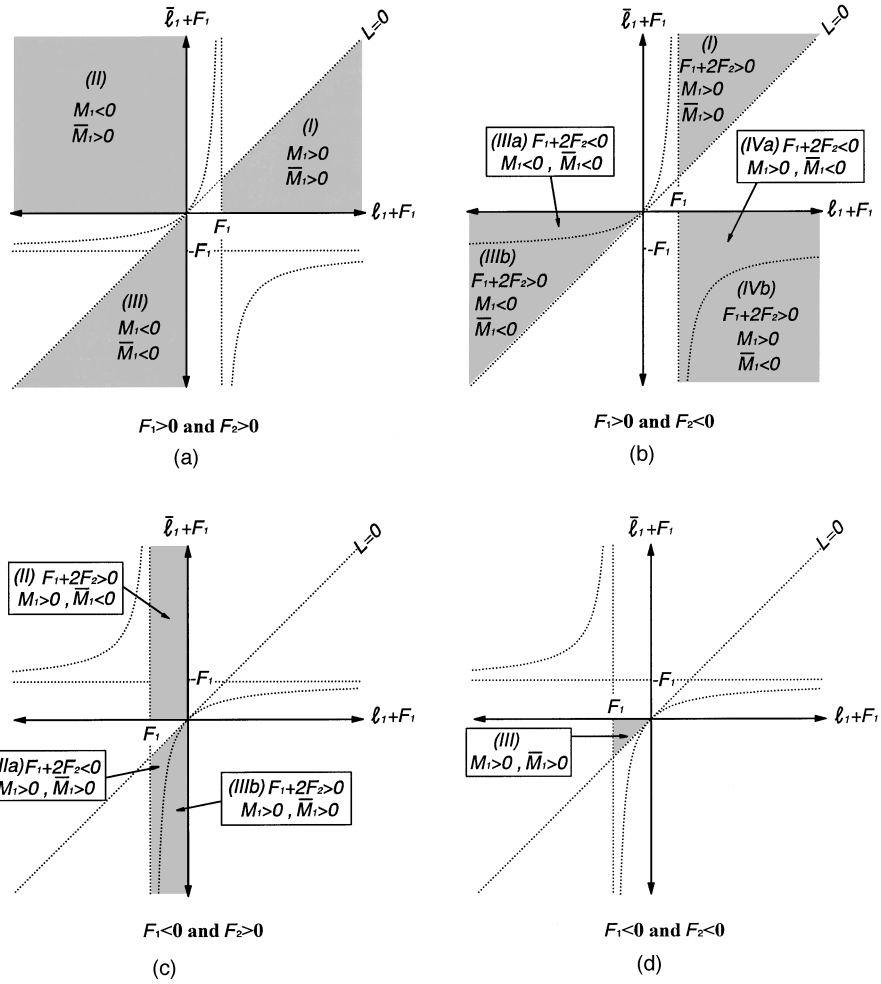

Fig. 3 Solution areas in the $\ell_1 \sim \bar{\ell}_1$ diagram are indicated with shadow regions: (a) to (d) show the solution areas for different combinations of F_1 and F_2 with the initial conditions $M_2=1$ and $M_2=-1$. The constraints on the signs of F_1+2F_2, M_1, and M_1 in each area are also shown. The value of L is positive at the upper-left section and negative at the lower-right section. The hyperbola represents the curves of $F_1+2F_2=0$.

age to the exit pupil, is positive in the upper-left section and negative in the lower-right section.

In Figs. 3 and 4, on the boundaries of solution areas the solutions of interlens separation may be zero or infinite and are not discussed here. If the solution points are on the hyperbolic curves in Figs. 3 or 4, we would have the results of $F_1+2F_2=0$ or $F_3+2F_2=0$.

2.2.2 *Case 2: $M_2=-1$ and $\bar{M}_2=1$*

In this case, the principal ray is through the center of the middle lens as shown in Fig. 5, Substituting $M_2=-1$ and $M_2=1$ into Eqs. (7) to (12), we get

$$F_2=\frac{M_1-\bar{M}_1}{2}F_1, \tag{31}$$

$$F_3=\frac{2}{1/M_3-1/\bar{M}_3}F_2, \tag{32}$$

$$d_{12}=(1-M_1)F_1+2F_2 \tag{33}$$

$$d_{12}=-\frac{F_1^2}{\ell_1+F_1}+(F_1+2F_2), \tag{34}$$

$$d_{12}=(1-\bar{M}_1)F_1, \tag{35}$$

$$d_{23}=2F_2-\left(\frac{1}{M_3}-1\right)F_3, \tag{36}$$

$$d_{23}=\frac{F_3^2}{\ell_3'-F_3}+(F_3+2F_2), \tag{37}$$

$$d_{23}=-\left(\frac{1}{\bar{M}_3}-1\right)F_3. \tag{38}$$

We also have the same equations as Eqs. (17) to (20),

$$\ell_1=\left(\frac{1}{M_1}-1\right)F_1 \tag{39}$$

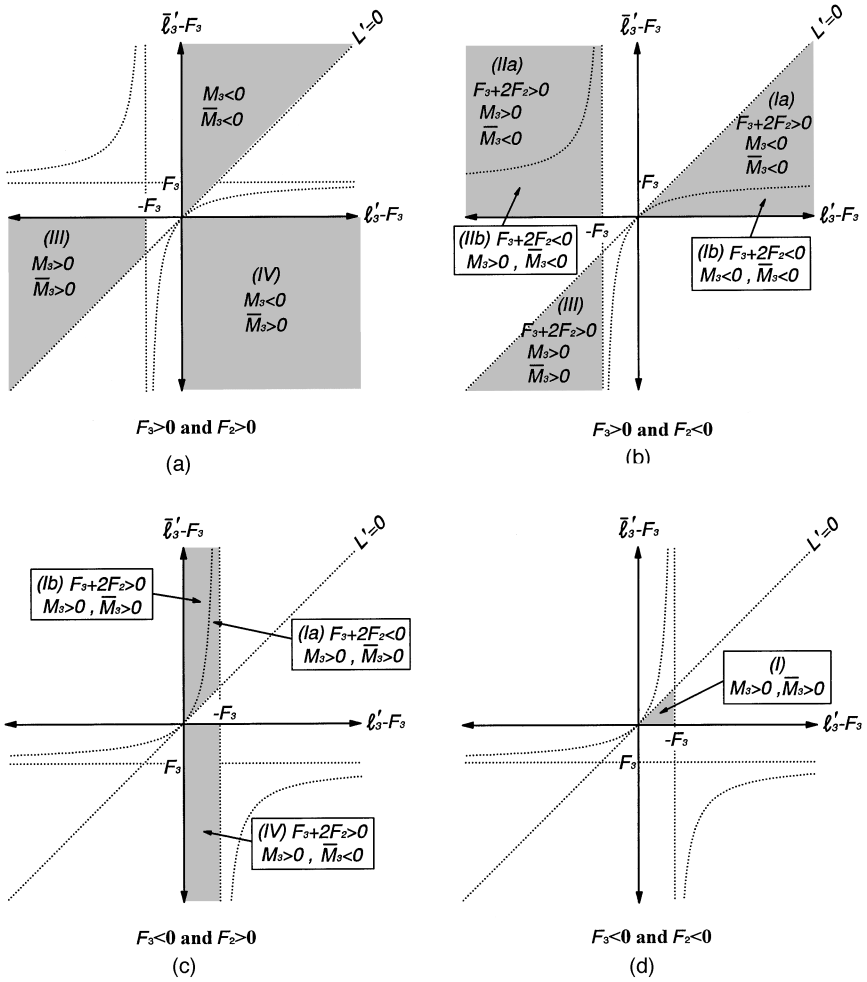

Fig. 4 Solution areas in the $\ell'_3 \sim \bar{\ell}'_3$ diagram are indicated with shadow regions: (a) to (d) show the solution areas for different combinations of F_2 and F_3 with the initial conditions $M_2=1$ and $M_2=-1$. The constraints on the signs of F_3+2F_2, M_3, and M_3 in each area are also shown. The value of L' is positive at the upper-left section and negative at the lower-right section. The hyperbola represents the curves of $F_3+2F_2=0$.

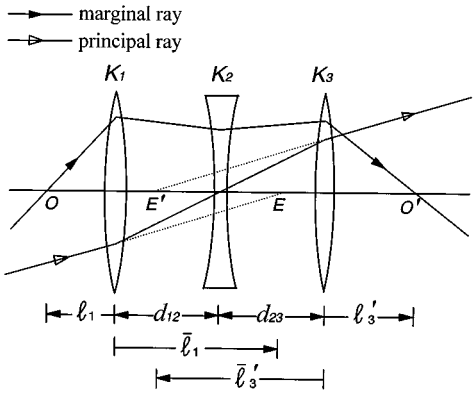

Fig. 5 Three-lens zoom system with the initial conditions $M_2=-1$ and $M_2=1$. The principal ray is through the center of the middle lens.

$$\bar{\ell}_1=\left(\frac{1}{\bar{M}_1}-1\right)F_1, \tag{40}$$

$$\ell'_3=(1-M_3)F_3, \tag{41}$$

$$\bar{\ell}'_3=(1-\bar{M}_3)F_3. \tag{42}$$

In the same way as we did in case 1, we get the solution ranges for ℓ_1, $\bar{\ell}_1$, ℓ'_3, and $\bar{\ell}'_3$, as listed in Tables 5 through 8. According to the different values of F_1, F_2, and F_3, the solution areas in the $\ell_1 \sim \bar{\ell}_1$ and $\ell'_3 \sim \bar{\ell}'_3$ diagrams are shown in Figs. 6 and 7.

Table 5 Solution ranges of entrance pupil position $\overline{\ell}_1$ for different types of F_1 with the initial conditions $M_2=-1$ and $M_2=1$.

Types of F_1	Solution Ranges of $\overline{\ell}_1$
$F_1>0$	$(\overline{\ell}_1+F_1)>F_1$ or $(\overline{\ell}_1+F_1)<0$
$F_1<0$	$F_1<(\overline{\ell}_1+F_1)<0$

2.3 *Interlens Separations d_{12} and d_{23} in Zooming*

To find the positions of the three lenses for a given magnification M during zooming, we must calculate d_{12} and d_{23}. From Eqs. (5) and (6) we have

$$d_{12}d_{23}=\frac{K\Delta-(K-K_1-K_2-K_3)d}{K_2(K_1+K_3)}. \tag{43}$$

Substituting $d_{12}d_{23}$ into Eq. (5), we have the relation of the interlens separations d_{12} and d_{23} as follows:

$$d_{23}=Ad_{12}+B, \tag{44}$$

where

$$A=-\frac{K_1(K_1K_2+KK_3)}{K_3(K_2K_3+KK_1)}, \tag{45}$$

and

$$B=\left(K_1+K_2+K_3-K+\frac{K_1K_3}{K_1+K_3}K\Delta\right)\frac{K_1+K_3}{K_3(K_2K_3+KK_1)}. \tag{46}$$

Table 6 Solution ranges of object position ℓ_1 for different combinations of F_1 and F_2 with the initial conditions $M_2=-1$ and $M_2=1$.

Types of F_1 and F_2		Solution Ranges of ℓ_1
$F_1>0$, $F_2>0$		$(\ell_1+F_1)>\frac{F_1^2}{F_1+2F_2}>0$ or $(\ell_1+F_1)<0$
$F_1>0$, $F_2<0$	$F_1+2F_2>0$	$(\ell_1+F_1)>\frac{F_1^2}{F_1+2F_2}>0$ or $(\ell_1+F_1)<0$
	$F_1+2F_2=0$	$(\ell_1+F_1)<0$
	$F_1+2F_2<0$	$\frac{F_1^2}{F_1+2F_2}<(\ell_1+F_1)<0$
$F_1<0$, $F_2>0$	$F_1+2F_2>0$	$(\ell_1+F_1)>\frac{F_1^2}{F_1+2F_2}>0$ or $(\ell_1+F_1)<0$
	$F_1+2F_2=0$	$(\ell_1+F_1)<0$
	$F_1+2F_2<0$	$\frac{F_1^2}{F_1+2F_2}<(\ell_1+F_1)<0$
$F_1<0$, $F_2<0$		$\frac{F_1^2}{F_1+2F_2}<(\ell_1+F_1)<0$

Table 7 Solution ranges of exit pupil position $\overline{\ell}'_3$ for different types of F_3 with the initial conditions $M_2=-1$ and $M_2=1$.

Types of F_3	Solution Ranges of $\overline{\ell}'_3$
$F_3>0$	$(\overline{\ell}'_3-F_3)>0$ or $(\overline{\ell}'_3-F_3)<-F_3$
$F_3<0$	$-F_3>(\overline{\ell}'_3-F_3)>0$

Using Eqs. (5) and (44), we find

$$d_{12}=\frac{-b\pm(b^2-4ac)^{1/2}}{2a}, \tag{47}$$

where

$$a=AK_1K_2K_3,$$

$$b=BK_1K_2K_3-AK_3(K_1+K_2)-K_1(K_2+K_3),$$

$$c=K_1+K_2+K_3-K-BK_3(K_1+K_2).$$

We substitute the given values of L, L', and P, which are from the initial position, into Eqs. (1) and (4) to get the values of K and $K\Delta$ as the functions of M. Then we can obtain the interlens separations with Eqs. (44) and (47) for each M value. After solving for d_{12} and d_{23}, we calculate the distance ℓ_1 from the first lens to the object and the

Table 8 Solution ranges of image position ℓ'_3 for different combinations of F_2 and F_3 with the initial conditions $M_2=-1$ and $M_2=1$.

Types of F_2 and F_3		Solution Ranges of ℓ'_3
$F_3>0$, $F_2>0$		$(\ell'_3-F_3)>0$ or $(\ell'_3-F_3)<\frac{-F_3^2}{F_3+2F_2}<0$
$F_3>0$, $F_2<0$	$F_3+2F_2>0$	$(\ell'_3-F_3)>0$ or $(\ell'_3-F_3)<\frac{-F_3^2}{F_3+2F_2}<0$
	$F_3+2F_2=0$	$(\ell'_3-F_3)>0$
	$F_3+2F_2<0$	$\frac{-F_3^2}{F_3+2F_2}>(\ell'_3-F_3)>0$
$F_3<0$, $F_2>0$	$F_3+2F_2>0$	$(\ell'_3-F_3)>0$ or $(\ell'_3-F_3)<\frac{-F_3^2}{F_3+2F_2}<0$
	$F_3+2F_2=0$	$(\ell'_3-F_3)>0$
	$F_3+2F_2<0$	$\frac{-F_3^2}{F_3+2F_2}>(\ell'_3-F_3)>0$
$F_3<0$, $F_2<0$		$\frac{-F_3^2}{F_3+2F_2}>(\ell'_3-F_3)>0$

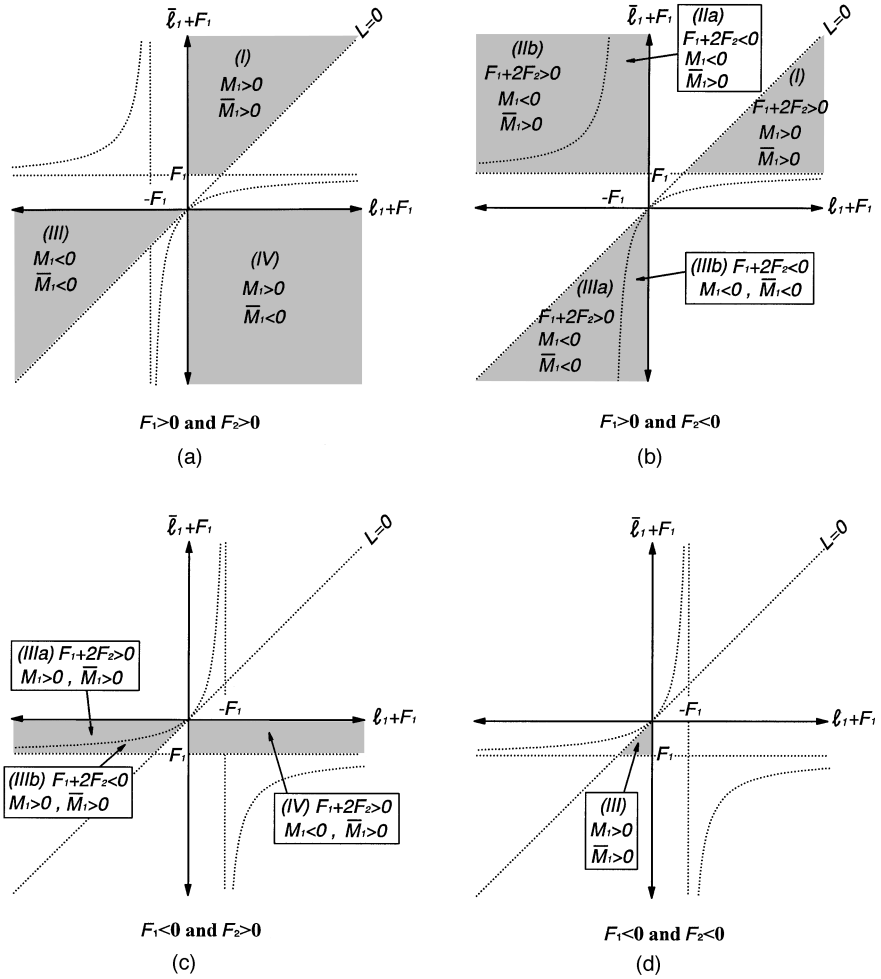

Fig. 6 Solution areas in the $\ell_1 \sim \bar{\ell}_1$ diagram are indicated with shadow regions: (a) to (d) show the solution areas for different combinations of F_1 and F_2 with the initial conditions $M_2=-1$ and $M_2=1$. The constraints on the signs of F_1+2F_2, M_1, and $\bar{M}_1$ in each area are also shown. The value of L is positive at the upper-left section and negative at the lower-right section. The hyperbola represents the curves of $F_1+2F_2=0$.

distance ℓ'_3 from the last lens to the image in any zooming position. In doing so, we need the values of δ (the distance from the first moving lens to the first principal plane H) and δ' (the distance from the last moving lens to the second principal plane H'), as shown in Fig. 1. These quantities can be calculated using

$$\delta = \frac{d_{23}K_3 + d_{12}(K_2 + K_3 - d_{23}K_2K_3)}{K}, \tag{48}$$

$$\delta' = -\frac{d_{12}K_1 + d_{23}(K_1 + K_2 - d_{12}K_1K_2)}{K}. \tag{49}$$

So ℓ_1 and ℓ'_3 are given by

$$\ell_1 = \ell + \delta, \tag{50}$$

$$\ell'_3 = \ell' + \delta', \tag{51}$$

where $\ell = (1/M-1)F$ and $\ell' = (1-M)F$.

3 Design Methods

To simplify the solving of a two-conjugate zoom system, we could give some related parameters in the initial position of zooming. If one of the two special initial conditions is selected as mentioned in Sec. 2.2, M_2 and M_2 will be determined. Besides, it can be seen from Eqs. (15) to (26) or Eqs. (31) to (42) that we still need the other five parameters, which could be the focal lengths of the three lenses, the object or entrance pupil distance from the first lens, the image or exit pupil distance from the third lens, the object/image or pupil magnifications of the first and third lenses, and the distance from object to image, etc. We propose two useful calculating procedures as follows.

3.1 *Given ℓ_1, $\bar{\ell}_1$, ℓ'_3, $\bar{\ell}'_3$, and F_1*

According to the system requirements and the expected signs of powers for the three lenses, we give the positions of the object, entrance pupil, image and exit pupil in the initial position and obtain the values of L and L'. One of the solution areas of Figs. 3 or 6 for ℓ_1 and $\bar{\ell}_1$ can be

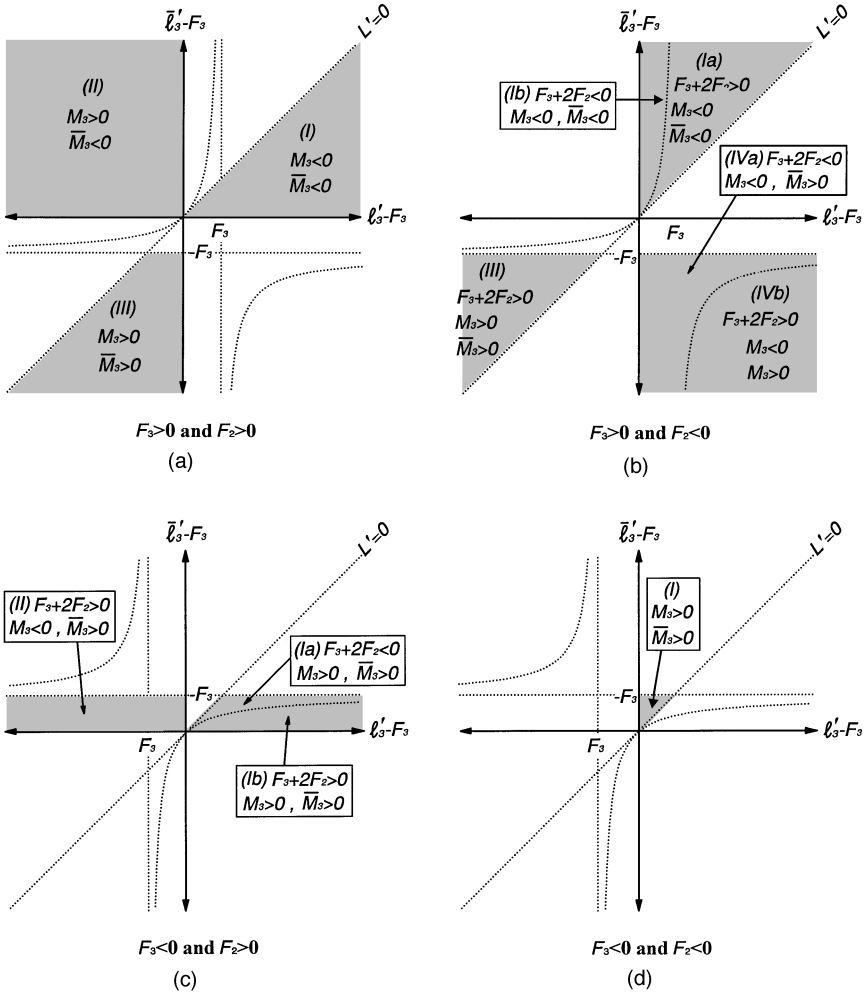

Fig. 7 Solution areas in the $\ell_3' \sim \overline{\ell}_3'$ diagram are indicated with shadow regions: (a) to (d) show the solution areas for different combinations of F_2 and F_3 with the initial conditions $M_2=-1$ and $M_2=1$. The constraints on the signs of F_3+2F_2, M_3, and M_3 in each area are also shown. The value of L' is positive at the upper-left section and negative at the lower-right section. The hyperbola represents the curves of $F_3+2F_2=0$.

chosen according to the given values of ℓ_1 and $\overline{\ell}_1$ and the expected signs of F_1 and F_2. The initial values of M_2 and M_2 depend on the selected initial conditions. We then choose a value of F_1 according to the constraint in the chosen solution area and calculate M_1 and M_1 from Eqs. (17) and (18) or Eqs. (39) and (40). The value of F_2 can be found from Eqs. (15) or (31). With Eqs. (2) and (3), we have

$$\frac{L'}{L}=M\overline{M}=M_1M_2M_3\overline{M}_1\overline{M}_2\overline{M}_3. \tag{52}$$

Combining this equation with Eqs. (19) and (20) or Eqs. (41) and (42), we have M_3 as follows:

$$M_3=\frac{-b\pm(b^2-4ac)^{1/2}}{2a}, \tag{53}$$

where

$$a=1,$$

$$b=\left(\frac{\ell_3'}{\overline{\ell}_3'}-1\right),$$

$$c=-\left(\frac{\ell_3'}{\overline{\ell}_3'}\right)\left(\frac{L'}{L}\right)\frac{1}{M_1M_2\overline{M}_1\overline{M}_2},$$

and $\overline{M}_3$ is given by Eq. (52). The value of F_3 is calculated from Eqs. (16) or (32). The interlens separations d_{12} and d_{23} are found from Eqs. (21) to (26) or Eqs. (33) to (38). The distance from object to image P is obtained from the following equation:

$$P=\left(2-M_1-\frac{1}{M_1}\right)F_1+\left(2-M_2-\frac{1}{M_2}\right)F_2 + \left(2-M_3-\frac{1}{M_3}\right)F_3. \quad (54)$$

If the initial structure is not satisfactory or the values of $\ell_3' - F_3$ and $\overline{\ell_3'} - F_3$ together with F_2 and F_3 are not located in the solution areas of Figs. 4 or 7 for ℓ_3' and $\overline{\ell_3'}$, we should adjust the related input parameters or choose another solution area. After obtaining the desirable result and the structure of zoom system under the initial condition, we can calculate the related parameters during zooming.

In zooming, the system magnification M changes; L, L', and P, which we have known from the initial position, remain constant. We can find K and $K\Delta$ with Eqs. (1) and (4) for any M value. We then find the interlens separations d_{12} and d_{23} from Eqs. (44) and (47), and the object and image distances ℓ_1 and ℓ_3' from Eqs. (50) and (51) during zooming. If the loci of the lenses are not smooth or the zoom ratio of the system is too small, of course, we can readjust the related input parameters or select the other initial condition.

3.2 *Given L, ℓ_1 (or $\overline{\ell_1}$), P, M, and F_1*

In practical design, the value of $L=(\overline{\ell_1}-\ell_1)$ is often given from the preceding system and the object/image distance P will also be a given value if the zoom lens is used as a relay system. In this case, if the object (or entrance pupil) distance from the first lens, ℓ_1 (or $\overline{\ell_1}$) is given, we will find $\overline{\ell_1}$ (or ℓ_1) from $L=(\overline{\ell_1}-\ell_1)$. The system magnification M may also be taken as an input parameter in the initial position. In this case, the value of M is often taken as 1 or -1. According to the given values of ℓ_1, $\overline{\ell_1}$, P, and M, and the expected signs of powers for the three lenses, we choose one of the solution areas of Figs. 3 or 6 for ℓ_1 and $\overline{\ell_1}$. Since the initial condition gives the values of M_2 and $\overline{M_2}$, we can calculate M_1 and $\overline{M_1}$ with Eqs. (17) and (18) or Eqs. (39) and (40) if a value of F_1 is given according to the constraint in the chosen solution area. We also find the value of F_2 from Eqs. (15) or (31) and obtain the focal length F_3 of the third lens from the following equations:

$$F_3=\left[P-\left(2-M_1-\frac{1}{M_1}\right)F_1-\left(2-M_2-\frac{1}{M_2}\right)F_2\right]\Bigg/ \left(2-M_3-\frac{1}{M_3}\right), \quad (55)$$

and

$$M_3=\frac{M}{M_1M_2}. \quad (56)$$

The $\overline{M_3}$ value is calculated with the following formulas:

$$P-L=\overline{P}-L', \quad (57)$$

$$\overline{P}=\left(2-\overline{M_1}-\frac{1}{M_1}\right)F_1+\left(2-\overline{M_2}-\frac{1}{M_2}\right)F_2 + \left(2-\overline{M_3}-\frac{1}{M_3}\right)F_3, \quad (58)$$

where $\overline{P}$ is the distance from entrance to exit pupil (EE') and we have

$$\overline{M_3}=\frac{F_3}{L-P+(2-\overline{M_1}-1/M_1)F_1+(2-\overline{M_2}-1/M_2)F_2+(2-M_3)F_3}, \quad (59)$$

ℓ_3' and $\overline{\ell_3'}$ are calculated from Eqs. (19) and (20) or Eqs. (41) and (42), and L' is then found from Eq. (14). The interlens separations d_{12} and d_{23} are obtained with Eqs. (21) to (26) or Eqs. (33) to (38). If the initial structure is not satisfactory or the values of $\ell_3' - F_3$ and $\overline{\ell_3'} - F_3$ together with F_2 and F_3 are not located in the solution areas of Figs. 4 or 7 for ℓ_3' and $\overline{\ell_3'}$, the related input parameters should be adjusted or another solution area should be chosen. In zooming, we obtain the interlens separations d_{12} and d_{23} and the object and image distances ℓ_1 and ℓ_3' with the procedures described in Sec. 3.1.

4 Examples

Using the method described, we design four different zoom systems. To obtain a zoom ratio R, the zoom system is usually arranged to have the overall magnification varied from $|M|=\sqrt{R}$ to $|M| = 1/\sqrt{R}$.

4.1 *Example 1: Given $\ell_1=90$, $\overline{\ell_1}=-130$, $\ell_3' = -80$, and $\overline{\ell_3'}=125$*

In this example, the object and image are virtual and the entrance and exit pupils are real in the initial position so that L is negative and L' is positive. We can find several possible solution areas in Figs. 3 and 6. If we expect that the zoom system comprises two positive lenses and a negative lens in between and has $M_2=1$ and $M_2=-1$ as the initial conditions, the solution area marked with (IVb) of Fig. 3(b) for ℓ_1 and ℓ_1 can be chosen. The calculation follows the procedures described in Sec. 3.1. If we give $F_1=50$, we obtain $M_1=0.357143$, $M_1=-0.625$, $M_3=2.64869$, $M_3=-1.576079$, $d_{12}=32.143$, and $d_{23}=30.204$ in the initial position. We also get $F_2=-24.5536$, $F_3=48.5234$, and the results of $F_1+2F_2>0$ and $F_3+2F_2<0$. The values of $\ell_3' - F_3$ and $\overline{\ell_3'} - F_3$ are located in the solution area marked with (IIb) of Fig. 4(b) for ℓ_3' and $\overline{\ell_3'}$. During zooming, the result is shown in Fig. 8, with the natural logarithm of $|M|$ as ordinate. The system has a zoom ratio of 16:1, magnification M from 4 to 0.25.

4.2 *Example 2: Given $\ell_1=-100$, $\overline{\ell_1}=-320$, $\ell_3' = 90$, and $\overline{\ell_3'}=295$*

In this case, we have different values of ℓ_1, $\overline{\ell_1}$, ℓ_3', and $\overline{\ell_3'}$ but the same $L=(\overline{\ell_1}-\ell_1)$ and $L' = (\overline{l_3'} - l_3')$, as compared with the previous example. Here, the object, image,

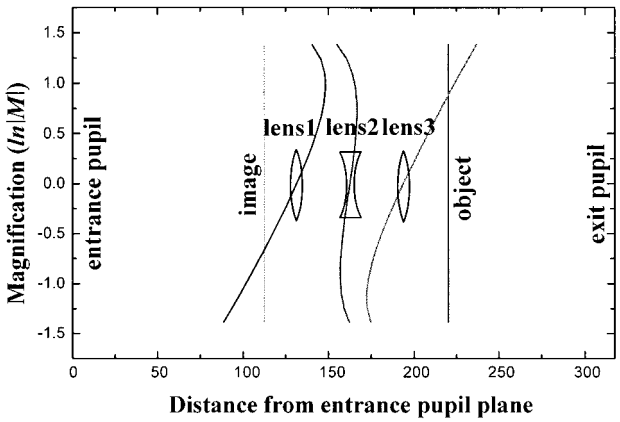

Fig. 8 Loci of three lenses in zooming. This system has virtual object and image with F_1=50, F_2=−24.5536, F_3=48.5234, and zoom ratio=16. The distance from object to image P is −107.654, the distance from entrance to exit pupil P is 317.347, and L=−220 and L'=205.

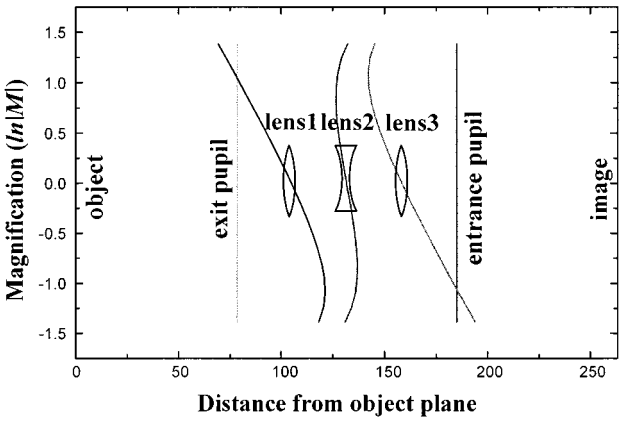

Fig. 10 Loci of three lenses in zooming. This system is symmetrical and has real object and image with F_1=40, F_2=−18.9744, F_3=40, and zoom ratio=16. The distance from object to image P is 263.333, the distance from entrance to exit pupil P is −106.667, and L=185 and L'=−185.

entrance, and exit pupils are all real. If the zoom system comprises two positive lenses and a negative lens in between and the initial conditions are chosen to be M_2=−1 and M_2=1, we can select the solution area marked with ($IIIa$) of Fig. 6(b) for ℓ_1 and ℓ_1. Following the procedures described in Sec. 3.1 and giving F_1=50, we obtain M_1=−1, M_1=−0.185185, M_3=−0.939344, M_3=−5.356738, d_{12}=59.259, and d_{23}=55.071 in the initial position. We also have F_2=−20.3704, F_3=46.4075, and the results of $F_1+2F_2>0$, $F_3+2F_2>0$. The values of $\ell'_3 - F_3$ and $\ell'_3 - F_3$ are located in the solution area marked with (Ia) of Fig. 7(b) for ℓ'_3 and ℓ'_3. During zooming, the result is shown in Fig. 9. The system has a zoom ratio of 16:1. The magnification M is from −4 to −0.25.

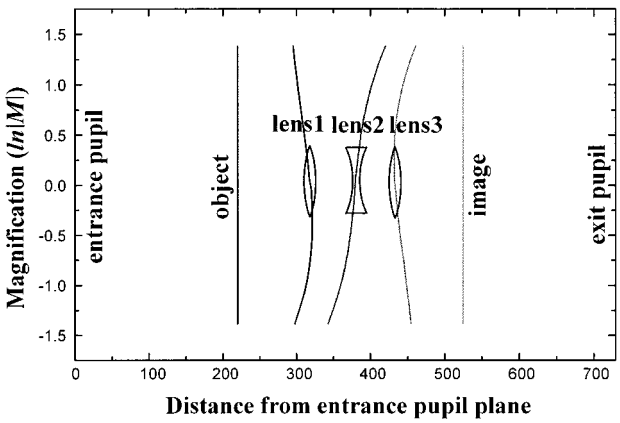

Fig. 9 Loci of three lenses in zooming. This system has real object and image with F_1=50, F_2=−20.3704, F_3=46.4075, and zoom ratio =16, and L and L' are the same as that in Fig. 8. The distance from object to image P is 304.330, and the distance from entrance to exit pupil P is 729.330.

4.3 *Example 3: Given ℓ_1=−105, ℓ_1=80, ℓ'_3 = 105, and ℓ'_3 = −80*

Here the object and image are real and the entrance and exit pupils are virtual in the initial position. From the given data, we have positive L, negative L', and $L=-L'$. If the system consists of two positive lenses and a negative lens located in between and the initial conditions give M_2=−1 and M_2=1, the solution area marked with (IIb) of Fig. 6(b) can be chosen. In the same way giving F_1=40, we obtain M_1=−0.615385, M_1=0.333333, M_3=−1.625, M_3=3, d_{12}=26.667, and d_{23}=26.667 in the initial position. We also have F_2=−18.9744, F_3=40, and the values of $\ell'_3 - F_3$ and $\ell'_3 - F_3$ located in the solution area marked with (IVb) of Fig. 7(b). In this example, the system is symmetrical and has $F_1=F_3$, $d_{12}=d_{23}$, $M_1=1/M_3$, and $M_1=1/M_3$ in the initial position. During zooming, the result is shown in Fig. 10. The system has a zoom ratio of 16:1. The magnification M is from −4 to −0.25.

4.4 *Example 4: Given L=195, ℓ_1=−105 (or ℓ_1=90), P=270, and M=−1*

In this case, the object is real and the entrance pupil is virtual in the initial position, so that L is positive. We expect that the system has two positive lenses and a negative lens in between. If we select the initial conditions in which M_2=−1 and M_2=1, we can choose the solution area marked with (IIb) of Fig. 6(b). Because M is −1, M_1 is equal to $1/M_3$ in the initial position. Following the calculating procedures described in Sec. 3.2 and giving F_1=42, we obtain M_1=−0.666667, M_1=0.318182, M_3=−1.5, M_3=3.299579, ℓ'_3 = 106.636, ℓ'_3 = −98.088, d_{12}=28.636, and d_{23}=29.727 in the initial position. We also have F_2=−20.6818, F_3=42.6545, and the results of $F_1+2F_2>0$, $F_3+2F_2>0$. The values of $\ell'_3 - F_3$ and $\ell'_3 - F_3$ are located in the solution area marked with (IVb) of Fig. 7(b). During zooming, the result is shown in Fig. 11. The system has a zoom ratio of 16:1 and the magnification M is from −4 to −0.25.

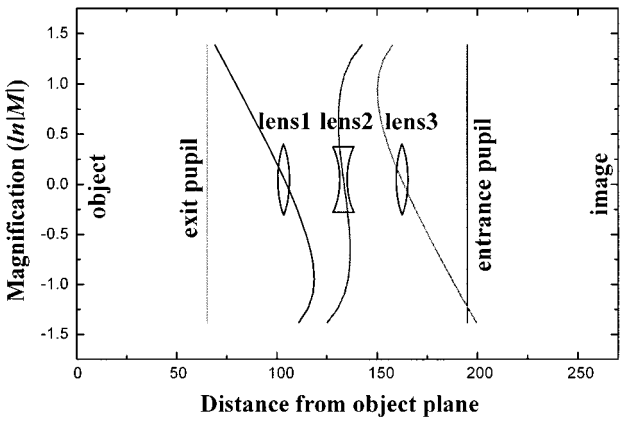

Fig. 11 Loci of three lenses in zooming. This system has real object and image with F_1=42, F_2=−20.6818, F_3=42.6545, and zoom ratio =16. The distance from object to image P is 270, the distance from entrance to exit pupil P is −129.724, and L=195 and L'=−204.724.

5 Discussion

For the first-order design of two-conjugate zoom lenses, we have analyzed the possible solutions for the positions of two pairs of conjugate planes that correspond to the object/image and pupils. The solution areas in the $\ell_1 \sim \ell_1$ and $\ell'_3 \sim \ell'_3$ diagrams are visual and helpful for designers to select the positive and negative types of three lenses in the zoom system and find the constraints on the powers of lenses if the values of ℓ_1, ℓ_1, ℓ'_3, and ℓ'_3 are given in the initial position. In this paper, we give F_1 and then calculate F_2 and F_3. Of course, instead of F_1, we can give F_3 and then calculate F_1 and F_2 with different design procedures. From Figs. 3 and 4 and 6 and 7, we find that the solution areas for negative first and third lenses are smaller than that for positive first and third lenses. Generally, Eqs. (47) and (53) should have two solutions. Sometimes only one of them can meet the conditions $d_{12}>0$ and $d_{23}>0$. However, if both the solutions meet these conditions, we will choose the solution that gives a better result.

In examples 1 and 2, two different results are obtained under the same values of L and L' but different values of M_2 and M_2, which correspond to the different initial conditions described in Sec. 2.2. We also find that the system in example 1 is more compact than that in example 2. In examples 1 to 4, the L and L' have opposite signs; this means that the direction from O to E is opposite to that from O' to E'. However, this is not a necessary condition in our design theory. Systems for different combinations of signs and values of L and L' can be solved only if the positions of two pairs of conjugate planes are located in the solution areas shown in the $\ell_1 \sim \ell_1$ and $\ell'_3 \sim \ell'_3$ diagrams. In many practical designs, we usually expect the initial condition is specified in the mean position of zooming, in which the system magnification M is +1 or −1. In this special case, we have one more constraint: $|M_1|$ is the reciprocal of $|M_3|$ due to $M=M_1M_2M_3$. The signs of M_1 and M_3 are the same or not depending on the sign of M_2, +1 or −1, such as in example 4. The formulas derived in this paper are suitable for the general two-conjugate zoom systems including the symmetrical systems described by Hopkins, who assumed $F_1=F_3$, $L=L'$, $\ell_1=-\ell'_3$, and $\ell_1=-\ell'_3$ in the mean position to be the necessary conditions. Example 3 is such a case.

6 Conclusion

As we know, a proper first-order layout often gives a satisfactory lens design. In general, the layout design of a two-conjugate zoom system is more difficult than that of an ordinary zoom system since both the entrance and exit pupils must be fixed during zooming. However, with the analysis of the solution areas in the 2-D diagrams for two pairs of the parameters (ℓ_1,ℓ_1) and (ℓ'_3,ℓ'_3), we can easily find the solutions for the two-conjugate zoom lens.

Acknowledgments

This project was supported by the National Science Council of the Republic of China under the grant No. NSC-85-2215-E-009-004.

References

1. A. Mann and B. J. Thompson, Eds., *Selected Papers on Zoom Lenses*, SPIE Milestone Series, Vol. MS 85, SPIE Press, Bellingham, WA (1993).
2. M. L. Oskotsky, ''Grapho-analytical method for the first-order design of two-component zoom systems,'' *Opt. Eng.* **31**(5), 1093–1097 (1992).
3. R. B. Johnson and C. Feng, ''Mechanically compensated zoom lenses with a single moving element,'' *Appl. Opt.* **31**(13), 2274–2278 (1992).
4. M. S. Yeh, S. G. Shiue, and M. H. Lu, ''Two-optical-component method for designing zoom system,'' *Opt. Eng.* **34**(6), 1826–1834 (1995).
5. H. H. Hopkins, ''2-Conjugate zoom systems,'' in *Optical Instruments and Techniques,* pp. 444–452, Oriel Press, Newcastle upon Tyne (1970).
6. S. G. Shiue, ''Gaussian optics for 2-conjugate zoom system,'' *Chinese J. Opt. Eng.* **2**(1), 17–21 (1985).

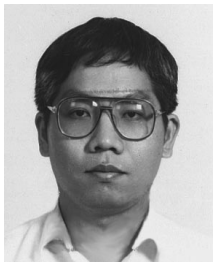

Mau-Shiun Yeh received his BS degree from the National Taiwan Normal University and his MS degree from the National Central University. Currently, he is pursuing a PhD at the Institute of Electro-Optical Engineering, National Chiao-Tung University. He was an assistant researcher with a major in optical lens design at the Chung Shan Institute of Science and Technology from 1986 to 1993.

Shin-Gwo Shiue received his BS and MS degrees from the Chung-Cheng Institute of Technology, Taiwan, in 1973 and 1976, and a PhD degree from the University of Reading, United Kingdom, in 1984. He became an assistant researcher at the Chung Shan Institute of Science and Technology in 1976. Before receiving his PhD degree, his research interest was mainly solid state laser physics and afterward concentrated in optical instrument design. He was a president of Taiwan Electro Optical System Company in 1990 and joined the Precision Instrument Developing Center of the National Science Council as a senior researcher in 1994. His current research is optical instrument developing, optical metrology, and lens design.

Mao-Hong Lu graduated from the department of physics at Fudan University in 1962. He then worked as a research staff member at the Shanghai Institute of Physics and Technology, Chinese Academy of Sciences, from 1962 to 1970 and at the Shanghai Institute of Laser Technology from 1970 to 1980. He studied at the University of Arizona as a visiting scholar from 1980 to 1982. He is currently a professor at the Institute of Electro-Optical Engineering, National Chiao-Tung University.